

DeepAlloc: CNN-Based Approach to Efficient Spectrum Allocation in Shared Spectrum Systems

Mohammad Ghaderibaneh
Stony Brook University
mghaderibane@cs.stonybrook.edu

Caitao Zhan
Stony Brook University
cbzhan@cs.stonybrook.edu

Himanshu Gupta
Stony Brook University
hgupta@cs.stonybrook.edu

ABSTRACT

Shared spectrum systems facilitate spectrum allocation to unlicensed users without harming the licensed users; they offer great promise in optimizing spectrum utility, but their management (in particular, efficient spectrum allocation to unlicensed users) is challenging. A significant shortcoming of current allocation methods is that they are either done very conservatively to ensure correctness, or are based on imperfect propagation models and/or spectrum sensing with poor spatial granularity. This leads to poor spectrum utilization, the fundamental objective of shared spectrum systems.

To allocate spectrum near-optimally to secondary users in general scenarios, we fundamentally need to have knowledge of the signal path-loss function. In practice, however, even the best known path-loss models have unsatisfactory accuracy, and conducting extensive surveys to gather path-loss values is infeasible. To circumvent this challenge, we propose to learn the spectrum allocation function directly using supervised learning techniques. We particularly address the scenarios when the primary users' information may not be available; for such settings, we make use of a crowdsourced sensing architecture and use the spectrum sensor readings as features. We develop an efficient CNN-based approach (called DeepAlloc) and address various challenges that arise in its application to the learning the spectrum allocation function. Via extensive large-scale simulation and a small testbed, we demonstrate the effectiveness of our developed techniques; in particular, we observe that our approach improves the accuracy of standard learning techniques and prior work by up to 60%.

1 INTRODUCTION

The RF spectrum is a natural resource in great demand due to the unabated increase in mobile (and hence, wireless) data consumption [3]. The research community has addressed this capacity crunch via the development of *shared spectrum paradigms*, wherein the spectrum is made available to unlicensed (secondary) users as long as they do not interfere with the transmission of licensed incumbents, i.e., primary users (PUs). Effective management (and in particular, allocation) of spectrum in such shared spectrum systems is challenging, and several spectrum management architectures have been proposed over the years [6, 7, 25, 38]. A significant shortcoming of these architectures and methods is that spectrum allocation is done very conservatively to ensure correctness, or is based on imperfect propagation modeling [10, 12] or spectrum sensing with poor spatial granularity. This leads to poor spectrum utilization, the fundamental objective of the shared spectrum systems. In this paper, we develop a learning-based approach to efficient allocation of spectrum in such shared spectrum systems.

Motivation and Overall Approach. In general, to allocate spectrum near-optimally to secondary users, we fundamentally need to have knowledge of the signal path loss between largely arbitrary pair of points. In practice, however, even the best known path-loss

models [12, 30] have unsatisfactory accuracy, and conducting extensive surveys to gather path-loss values is infeasible and moreover, may not even reflect real-time channel conditions. To circumvent the above challenge, we propose to instead learn the spectrum allocation function directly using supervised learning techniques. In scenarios where primary-user (PU) parameters may not be available (e.g., navy radars in CBRS band [1]), we use a crowdsourced sensing architecture where we utilize relatively low-cost spectrum sensors independently deployed with a high granularity [9, 11, 23, 35]. A sensing architecture also enables spectrum allocation based on real-time channel conditions [15].

We propose to use supervised learning techniques to learn the Spectrum Allocation (SA) function with the input (features) being the primary-user parameters, spectrum sensor (SS) readings, and secondary user (SU) request parameters, and the output (label) being the maximum power that can be allocated to the SU without resulting in any harmful interference to the PUs' receivers. Apart from the standard supervised schemes such as linear regression, artificial neural networks, and support vector regression (SVR), we propose using a convolution neural network (CNN) based model to learn the spectrum allocation function. CNN model is a widely used approach for image classification. CNN is particularly suited to our context due to the spatial nature of our setting. To develop an overall effective CNN-based technique, we need to develop techniques to represent the inputs to the SA function as an image, design an efficient CNN architecture, and address associated challenges.

Our Contributions. We make the following contributions.

- (1) We motivate a supervised learning-based approach for efficient allocation of spectrum to secondary users in a shared spectrum system. In particular, we propose the use of Convolution Neural Networks (CNN) for efficient learning of the spectrum allocation function.
- (2) We develop an efficient CNN architecture based on *pre-training* a deep model using a large number of *auto-generated* samples/images, followed by training using samples gathered over the given region.
- (3) To make our CNN architecture effective in learning the spectrum allocation function, we develop techniques to transform training samples into images as input to our CNN models, minimize false positive errors, handle multi-path effects, and further improve accuracy via synthetic samples.
- (4) We evaluate our techniques using large-scale simulations as well as an outdoor testbed, and demonstrate the effectiveness of our developed techniques. We observe that our approach improves the accuracy of other approaches by up to 60%.

2 PROBLEM, RELATED WORK, AND OUR APPROACH

Shared Spectrum Setting. As mentioned before, a shared spectrum system mainly consists of licensed primary users (PUs) and

unlicensed secondary users (SUs) who make spectrum allocation requests to the centralized *spectrum manager* (SM). For a given SU request, the goal of the spectrum allocation algorithm is to allocate maximum possible power to the SU such that its transmission at the allocated power would not interfere with PU's reception at any of its receivers. However, in practice, PU parameters may not be available, e.g., in the CBRS 3.5GHz shared band [1] wherein the licensed users include Navy radar systems. For such settings, we propose to make use of a crowdsourced sensing architecture where relatively low-cost spectrum sensors are independently deployed with a high granularity [9, 11, 23, 35]. This approach also enables spectrum allocation based on real-time channel conditions [15]. In such a crowdsourced sensing architecture, allocation decision is based on the readings of deployed sensors.

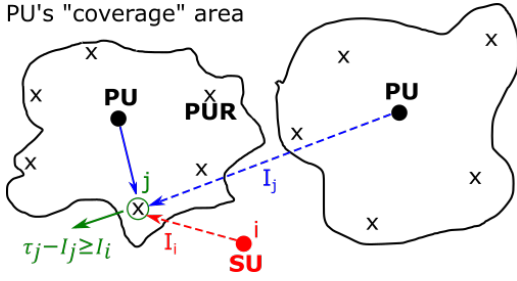


Figure 1: Spectrum Power Allocation (Eqn. 1). Optimal power that can be allocated to an SU is such that the interference caused is less than the "residual" threshold $\tau_j - I_j$ at each PUR R_j ; here, τ_j is PUR's initial threshold and I_j is the total interference at the PUR from other PUs.

Spectrum Allocation Function/Algorithm. Consider a shared spectrum area where PUs (and their receivers) and/or a set of SUs are deployed. We assume a single channel throughout this paper (multiple channels are handled similarly (§3.6)). To access the spectrum, SUs send requests to the SM, which then determines the power level at which the SU can access the spectrum such that no interference is caused to any of the PUs' receivers. There are many ways to model PU receivers, e.g., a coverage region around PU. Here, as in [21, 24], we assume a finite set of representative receivers called PURs around a PU. Each PUR is associated with an *initial threshold*, which is continually updated, to signify the maximum additional interference it can tolerate from the other PUs and SUs. To formulate the problem mathematically [15, 17, 21], let us denote the path loss function by $\rho(\cdot, \cdot)$. Then, if a SU S_i at location l_i is allowed at power t_i , the signal power received at PUR R_j at location l_j is given by $p_{ij} = t_i \cdot \rho(l_i, l_j)$. Let the total interference from other PUs at R_j be I_j . To ensure that $p_{i,j} + I_j$ is less than each R_j 's current threshold τ_j , the maximum power Π that can be allocated to the SU is:

$$\Pi \leq \min_j \frac{\tau_j - I_j}{\rho(l_i, l_j)} \quad (1)$$

Once a certain transmit power t_i has been allocated to a SU S_i , the threshold for a PUR at location l_j is updated to: $\tau_j = \tau_j - t_i \times \rho(l_i, l_j)$, to account for the interference caused by S_i due to the assigned power. Thus, for a single SU request, a plausible spectrum allocation function/algorithm may consist of the following steps: (i) compute

the path loss between the SU and each of the PURs, (ii) allocate spectrum as per Eqn. 1, (iii) update the PURs' threshold. This is the spectrum allocation function assumed throughout this paper.

2.1 Related Work

The spectrum allocation problem has been studied extensively (see [19, 38, 46] for survey), especially in the context of shared spectrum systems. In a centralized SM architecture, it is generally assumed that the SM has complete knowledge of the PU parameters. Many prior works also assume a propagation model which, in conjunction with known PU parameters, allows spectrum allocation power to be computed via linear programming [38] or other simple techniques for common optimization objectives. However, in practice, PU parameters may not be available, e.g., in the CBRS (3550-3700 MHz) in the 3.5GHz band [1] wherein the licensed users include Navy radar systems. As most propagation models have unsatisfactory accuracy, spectrum allocation must be done overly conservatively for correctness. In particular, in TV white spaces spectrum (54-698 MHz) [2], spectrum allocation is done based on a database with TV channel availability at each location; in essence, the SU is allowed to transmit with a certain power, if the signal received at its location is below a low threshold. Such a **listen-before-talk** [27, 37] allocation strategy in general can be very conservative due to a combination of reasons: (i) the observed signal is actually an aggregate over all PUs in the same band, (ii) path-loss need not be symmetric, (iii) SUs may want to transmit at a much lower power than the PUs, and (iv) PURs may be a distance away from the PUs. In static systems, a database approach [1] can also be used by pre-computing the SA function and storing in the databases; however, such an approach doesn't work in any dynamic situation, e.g., SUs in tertiary level, PUs changing powers, path-loss changes due to real-time conditions. In a closely related work, [21] has developed an interpolation-based spectrum allocation scheme that works by first estimating the desired path-loss values based on signal strength readings from deployed spectrum sensors. In particular, they use inverse-distance weighted and Ordinary Kriging interpolation schemes to estimate the path-loss values. We compare our approach with theirs in §4-§5.

Machine Learning (ML) Based Approaches. To the best of our knowledge, there have been no prior works that have used supervised learning to directly learn the SA function, especially as defined here. The closest work is [4] which uses supervised learning to analyze spectrum *occupancy* based on the sensed signal at the SU. Some works [31, 42] have used reinforcement learning (RL) techniques for applications wherein the goal is to maximize *cumulative* spectrum utilization over time by exploiting arrival patterns of the SUs. In contrast, our goal is to allocate the maximum power to the *current* SU request, in applications with no underlying pattern of SU requests/arrivals. RL techniques may be useful in handling *simultaneous* SU requests; in our work, we handle simultaneous requests one at a time (see §3.6). There have also been some works [39] on learning the path-loss function, which can then be used to allocate spectrum using Eqn. 1. However, Eqn. 1 requires knowledge of PU parameters, which may not be available. Moreover, the path-loss function fundamentally encodes more information than the SA function, and thus, would likely require

much more training. In other works, H. Zhang et al. [45] propose a deep RL algorithm where a deep Neural Network is used to help SUs to obtain information about PUs' power policies. SU power is adjusted in a non-cooperative (with PUs) manner until its QoS requirement is satisfied. Authors in [13] propose a distributed multi-agent reinforcement learning based joint spectrum allocation in device-to-device communications to maximize overall throughput. More recently, Zhan et al. [44] propose a CNN-based approach to efficiently locate the users in a crowdsourced sensor network.

Multiple Channels and Other Objectives. In this paper, we implicitly assume a single channel for the most part. Spectrum allocation for multiple channels can be done by using single-channel techniques independently for each channel and then selecting one of the available channels based on some criteria (see §3.6). For example, H. Wang et al. [40] picks a channel that maximizes the aggregate data rate of SUs, and X. Li et al. [28] picks a channel that allows for minimum transmission power for a desired SU data rate. Other works have addressed spectrum allocation with other optimization objectives. e.g., researchers have considered throughput maximization as an objective [33, 41] under various constraints such as maximum allocated power [28], given QoS requirements [26], etc. Fairness and energy efficiency are some other criteria considered [8, 20, 43].

2.2 Our Learning Approach

Motivation. Our goal is to allocate spectrum efficiently to SUs in general settings, e.g., when PU parameters may not be available. To motivate and justify our learning based approach, we make the following remarks. First, we note that to allocate spectrum near-optimally to secondary users in general scenarios, we fundamentally need to have knowledge of the signal path-loss function. In practice, however, even the best known path-loss models [12, 30] have unsatisfactory accuracy, and conducting extensive surveys to gather path-loss values is infeasible and moreover, may not even reflect real-time channel conditions. In absence of knowledge of a path-loss function, to allocate spectrum efficiently, we propose to just learn the spectrum allocation function directly using supervised learning techniques. Second, in our context, an unsupervised approach is meaningless as unlabelled samples have minimal information (actually, zero information in the PU-Setting; see below). As explained in the previous subsection, a reinforcement-learning approach is also not suitable for our specific setting. Finally, learning the path-loss function first and then using Eqn. 1 to allocate spectrum is certainly a feasible approach – but, since the path-loss function fundamentally encodes more information than the SA function, it would likely require much more training (note that the SA function depends only on the most restrictive of the PURs).

Based on the above analysis, we learn the SA function directly from training over PU parameters and/or SS parameters (e.g., when PU parameters are unknown). In general, we wish to learn the SA function accurately with minimal training, even when the PU parameters may not be known. Below, we discuss the various types of inputs/features available and thus the two settings considered in our work, and the training process of gathering the samples.

Features of the SA Function \mathcal{A} . For most of the discussion in this paper, we focus on spectrum allocation to a *single/first* SU in a given area; multiple or subsequent SUs can be handled similarly as

discussed later in §3.6. In the simplest of settings, the PUs' information/parameters (location and transmit power) do not change over time, and hence the SA function can be simply represented as $\mathcal{A}(l)$ as the fixed PU parameters will be automatically captured within the learned model. In this work, we focus on the more general settings wherein the PUs' information (location and power) may change over time (i.e., across training and evaluation samples). In particular, we consider two settings: (i) if the PU parameters are known (for every sample), or (ii) if the PU parameters are not known (in which case, we need to use spectrum sensors). We refer to them as PU-Setting and SS-Setting respectively as described in more detail below.

- (1) PU-Setting. In this setting, we can represent the SA function $\mathcal{A}(\mathcal{R}, l)$ as a real-value function of PU parameters \mathcal{R} and location l of the requesting SU. The PU parameters essentially include its location, transmit power, and the PURs' locations (and thresholds).
- (2) SS-Setting. In this setting, we must include parameters from the deployed Ss as features, and represent the SA function as $\mathcal{A}(\mathcal{S}, l)$, where \mathcal{S} is the set of SS parameters; for each SS, its parameters may include its location and aggregate received power from the PUs (but in general, the mean and variance of the Gaussian distribution of the received power). Allocation based on SS parameters is implicitly based on *real-time* channel conditions, which is important for accurate and optimized spectrum allocation, as the conditions affecting signal attenuation (e.g., air, rain, vehicular traffic) may change over time.

Gathering and Labeling Training Samples. Note that gathering a training sample for \mathcal{A} entails gathering feature values and determining its "label"—in our context, for a given feature vector (SU location and PU parameters), the label is the maximum power that can be allocated to the SU without causing harmful wireless interference at *any* of the PURs. There are two ways to achieve this: (i) Compute the path-loss between SU and each PUR, and then use Eqn. 1; (ii) Deploy and simulate SU and PURs, and see if each PUR receives its PU's signal with the desired signal strength (as in our testbed; see §5). When PU parameters are unavailable, we would need to also simulate PUs. Either of the above training processes can incur a substantial cost, but can be automated using drones for entities. Note that the training is done only one-time, and thus, some amount of training cost is feasible.

3 CNN-BASED DEEP LEARNING APPROACH

Due to the spatial nature of the SA problem, the whole setting with its elements (e.g. SUs, PUs) can be represented as a 2D image. This representation gives us the leverage to use Convolutional Neural Network (CNN) which are best suited for learning over image input data (and in general, over spatial data). In this section, we motivate CNN's suitability for our context, and design an efficient CNN architecture and associated techniques for our problem.

CNNs. CNNs is a deep learning algorithm that has proved its ability to successfully capture the spatial and temporal dependencies among objects [47] in an image. The input data needs to be represented as a multidimensional data array; e.g. images can be represented as a 2D array of pixel values, videos can be represented in a

3D structure, etc. Then, a series of *convolution layers* consisting of *filters* (learned through *back-propagation*) extract several abstract features, with the output of the last convolution layer "flattened" to feed into *fully-connected layers*. CNN has been largely used to classify images or to analyze visual imagery existing in images. CNN can be efficient in detecting shapes and objects in images by first detecting smaller parts and then spatially correlating them to classify bigger objects. Thus, the higher layers work with inputs with less lower-level details but with more high-level information (detected features).

CNN-Based Spectrum Allocation. The geographical nature of the SA function suggests that CNN is well-suited for learning the function. In particular, the features of the SA function can be represented in a image, and then learning the function using CNNs could leverage the spatial correlation among the input features. In particular, CNNs are able to exploit the spatial structure via the use of learnable filters (or kernels) in the convolution layers. However, there are significant challenges that need to be addressed, to make CNN a viable and efficient approach to learn the SA function. These include the pre-processing of samples into "images" to feed as input to a CNN model, creating an efficient CNN architecture, ensuring minimal false positives, handling multi-path fading effects, minimizing training cost, etc. We discuss these challenges in the following subsections.

3.1 SH-Alloc: Shallow CNN Model

In this subsection, we discuss our basic CNN architecture and approach, which we refer to as SH-Alloc, as it has a small number of layers. In the next subsection, we will extend this approach to the DeepAlloc approach that uses a much deeper CNN architecture with a larger number of layers. We start with discussing our strategy to pre-process training samples into images.

Pre-Processing Training Samples to Images. The first challenge in applying CNNs to our context effectively is to transform each training sample to an "image" for input to the CNN model, in a way that it is most conducive to efficient learning. Representing the entities (PUs, SSs, SUs) as objects in a 2D image is a natural choice. In particular, we could represent each entity type with a different color or shape, or more specifically, represent each entity by a disk of a certain color with a radius based on the transmit/received power. Our choice of image representation is tantamount to *feature engineering* [5], and can have a significant impact on the training cost. Below, we discuss the choice made in our model design. We assume that the distribution of PURs around PUs is uniform, and thus, the PURs do not need to be represented in the image. Also note that we don't need to represent PUs and SSs together, as per the two problem settings PU-Setting and SS-Setting.

Representing PUs in Multiple Image "Sheets." Note that just using shapes or colors for different entities is not sufficient, as we also need to represent transmit/received powers. Just using radius to represent powers is not viable either, as we may start getting intersections between shapes. Thus, we compose the input image of a certain number of "sheets" (see Figure 2). Then, we divide the expected transmit-power range into smaller ranges, and assign each PU to the appropriate image sheet depending on its transmit power. Within each sheet, we then use disks to represent each

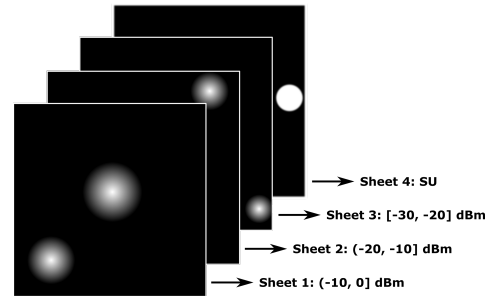


Figure 2: Image representation of a sample for input to the DeepAlloc model. Here, there are four PUs (2 in the first sheet, and 1 in the other two sheets) and one SU (in the fourth sheet). Each sheet for the PUs corresponds to a range of PU's transmit power; e.g., PUs whose transmit power is in the range -10 to 0 dBm are placed in the first sheet.

PU, with the brightness of the center pixel as well as the radius of disk proportional to the transmit power. In addition, to give more importance to the center (which represents the true location) and to suggest signal attenuation away from the center, we decrease the brightness of the pixels away from the center in a logarithmic manner. If there is an intersection between two objects in the same sheet, we aggregate the intensity of the common pixels. Unlike normal images which are composed of three sheets corresponding to red, green, and blue colors, we may use more than three sheets.

Representing SUs and SSs. Another benefit of using image sheets is that we can assign a separate sheet to represent SU(s)—instead of representing them with a different shape/color. SSs can be represented similar to PUs with the size of their disk proportional to the *received* (rather than transmit) power; note that, in our context, we don't need to represent PUs and SSs together, but, if information from both PUs and SSs is available, they can be represented in different sheets. We choose the radius of the SSs to be smaller than that of PUs as the density of SSs in an area is expected to be much more than the PUs to avoid many intersections among the disks.

Overall Pre-Processing Approach. Thus, our overall approach to pre-process a training sample consists of the following steps:

- (1) Divide the expected transmit (received) power range of PUs (SSs) into P sub-ranges each of about 5-10dBm.
- (2) Create an image input with P sheets to represent PUs (or SSs) and one for the (single) SU request.
- (3) For each PU (or SS), create a disk in the corresponding sheet at its location, with the disk's center brightness and radius both proportional to its transmit (received) power, and the intensity of the pixels decreasing from the center in a logarithmic manner.
- (4) For the given SU request, create a solid disk at the SU location of uniform intensity in the last sheet of the image. The radius of SU's circle is fixed across training and evaluation samples to aid the model to detect the SU's location efficiently.

SH-Alloc CNN Model Architecture. To design a CNN architecture to learn the SA function efficiently, we need to carefully determine the various *hyper-parameters*, e.g. number of convolution and fully-connected layers, number and size of filters, regularization parameters, activation functions, etc. For our SH-Alloc model,

we choose these parameters as follows. **(i)** Number of convolution layers in a CNN model plays an important role in training cost as well as model accuracy. In general, a deeper model (i.e., with more number of convolution layers) performs better than a shallow one but incurs more training cost. In our context, only a few thousand training samples being feasible to gather, we use 5 convolution layers, and 3 fully-connected layers as in a neural-network architecture. **(ii) Filter Size:** To be able to "detect" small-radii PUs of small power values, we use a 3×3 filter in the convolution layers. The number of filters is small for the initial layers, and then increases with the "depth"; this facilitates the detection of more and more complicated features in the deeper layers. **(iii) Activation Function:** In our context, as the final output of the model is a real number, we chose a linear activation function for the last network layer with only one neuron. For other layers, we use Rectified Linear Units (ReLU) [32] activation function as its non-linearity enables the model to learn a more complex function faster.

The overall CNN-based spectrum allocation system is shown in Fig. 3, including components discussed in the following subsections.

3.2 DeepAlloc: Pre-Trained Deep CNN Model

It is well understood that deeper neural networks, i.e., neural networks with more layers, and in particular, deeper CNN models can yield much better performance with their ability to learn more complex functions, with sufficient training data. However, there are two major challenges with using deep models. First, as the number of layers increase, so does the number of parameters to learn—which in turn requires a much larger number of training samples. Second, a deeper model is more likely to learn a function that overfits the training data, if the training data is not sufficient. The perfect solution is to use a deep network but also have a sufficiently large training set. However, in our context, it is infeasible to gather more than a few thousand samples as the deployment and/or labelling costs are high, while a very deep (e.g., with 20-100 layers) network may require close to a million samples to train properly [14, 22, 36].

Using Pre-Trained Models. Our approach to address the above challenge is to use a *pre-trained* deep model, i.e., a deep model that has already been trained with readily-available images, which may not represent spectrum allocation samples. Such a strategy has been often used in computer vision applications with great success. Similarly, we could also use pre-trained deep well-known models such as VGG [36], ResNet [22], Xception [14] which have been trained with around 1 million daily-life images, and then train them further with a few thousands of spectrum allocation training samples, as in the previous subsection.

DeepAlloc Approach. One unique aspect of our context is that the pre-training samples or images can be easily synthesized based on an assumed propagation model. Thus, to obtain better performance than the above models pre-trained with daily-life images, we can pre-train a deep architecture (we used VGG [36]) with generated spectrum allocation images based on an assumed log-normal propagation model with an "appropriate" path-loss exponent. The path-loss exponent α can be derived by gathering a few (say 100-200) path-loss samples, and determining the best α that minimizes the error between the actual path-loss samples and those from the log-normal model. See Fig. 4. Then, as before, we train such a

pre-trained model further with a few thousands of spectrum allocation training samples as shown in Fig. 3. We refer to this overall approach as DeepAlloc.

3.3 Minimizing False Positive Error

Recall that the power allocated to the SU should be such that SU transmission at the allocated power doesn't cause harmful interference to the PU receivers. In our context of a shared spectrum system, this constraint or condition is strict – i.e., a spectrum allocation algorithm should almost never allocate a power higher than the optimal power, where the optimal power is the one determined by Eqn. 1. We term the cases where our model returns a power higher than the optimal as *false positive* cases. In essence, we want to minimize the false positive cases drastically – perhaps, at the cost of higher number of (and/or errors in) the false negative cases. We address this issue by a combination of two strategies. First, we choose the hyper-parameters of the CNN model in a way that minimizes the number of false positives; the methodology here is largely trial and error, due to lack of techniques to systematically search for hyper-parameter values. Second, we use asymmetry in the training loss function as follows. Essentially, we change the training loss function $\mathbf{J}(\theta)$ such that false positive samples (an SU requests that gets higher power than the maximum) be penalized more drastically than the other requests. More formally, we define the training loss function as:

$$\mathbf{J}(\theta) = \frac{1}{m} \left(\alpha_{FP} \sum_{\hat{y}_i > y_i} l(\hat{y}_i, y_i, \theta) + \alpha_{FN} \sum_{\hat{y}_i \leq y_i} l(\hat{y}_i, y_i, \theta) \right) \quad (2)$$

Above, α_{FP} and α_{FN} are coefficient weights for the false positives and false negatives respectively, y_i is the "ground truth", \hat{y}_i is the predicted value, θ is the internal set of the parameters being learned, and $l(\cdot)$ defines the error for a single sample. To minimize false positives, we can choose a much higher α_{FP} than α_{FN} .

3.4 Handling Multi-Path Effect

Wireless signal attenuation is a result of three mutually independent, multiplicative propagation phenomena [34], viz., large-scale signal attenuation, medium-scale shadowing, and small-scale multipath fading. The shadowing effect can cause overall path-loss to vary over 10s to 100s of meters, and the fading effect can cause an effect over a few wavelengths. See Fig. 5 (a). The overall effect of these phenomena in our context is that learning the SA function could require a much higher number of training samples—to sufficiently and accurately capture the small to medium scale fluctuations. This challenge is fortunately mitigated by the fact that the small-scale fluctuations in the path-loss function are unlikely to fully manifest in the SA function, as the SA function depends only on the most restrictive of the SU-PUR path losses.

In our context, one way to address the above challenge is to learn instead of a more "conservative" SA function that may be easier to learn but may allocate sub-optimal power. E.g., the conservative SA may be based on a *lower-bound* approximation of the path-loss function. See the red curve in Fig. 5 (a). We note that the technique in the previous section is also driven towards learning a more conservative function via an appropriate training loss function. However, the model inaccuracy resulting from the multi-path effect

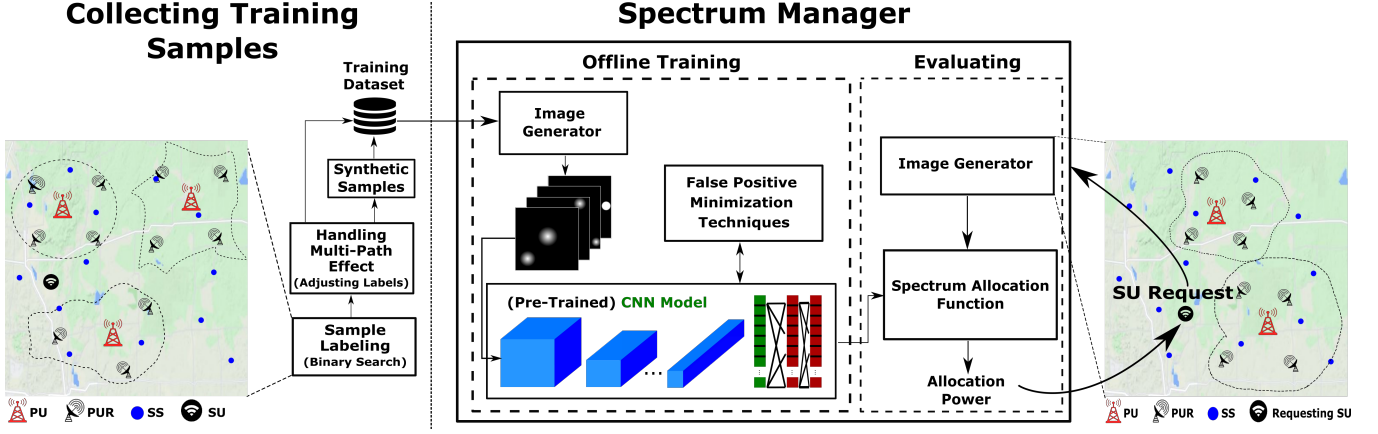


Figure 3: CNN-based Spectrum Allocation System. For the CNN Model component, SH-Alloc uses a shallow CNN model without any pre-training, while DeepAlloc uses a deep pre-trained CNN model obtained from Fig. 4. In both cases, after any pre-training, the (field) training samples are gathered, converted into images, and then used to (further) train the CNN model. The learned model is then used to allocate spectrum to requesting SUs.

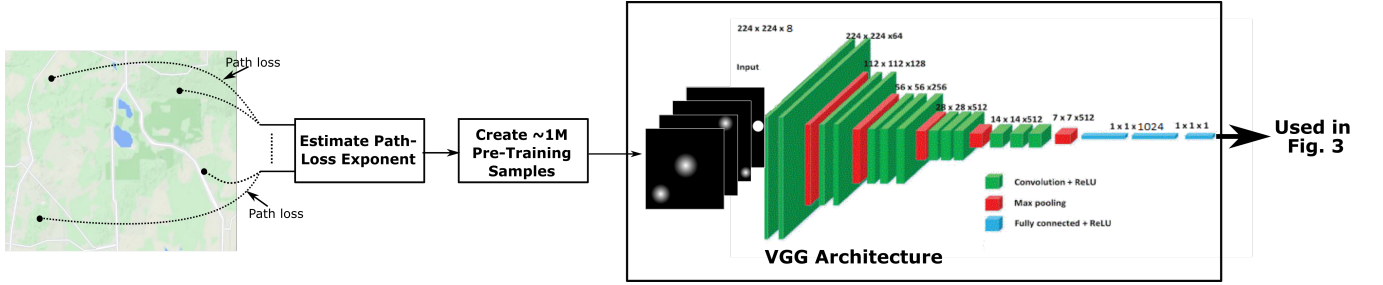


Figure 4: DeepAlloc Pre-Training Process. Here, we generate a large number ($\approx 1M$) of images assuming a log-normal propagation model based on an estimate path-loss exponent, and pre-train a deep CNN model using these generated images. The pre-trained model is then used in Fig. 3 for further training using a smaller number of field training samples.

is fundamentally due to a lack of sufficient training samples needed to learn a function with high spatial resolution/variability; thus, we can't fix the model inaccuracy due to the multi-path effect by merely changing the loss function, model, or its training process. Our strategy to learn a more conservative function that addresses the multi-path effect challenge is to actually modify the labels of the training samples appropriately, as discussed below.

Learning a Conservative SA Function by Modifying Training Sample Labels. To ensure few false positives in face of the small-scale multi-path fading effect, we modify the training samples by lowering their labels from the optimal allocated power to smaller values so that the modified training samples represent a "conservative" spectrum allocation function without the small-scale effects. In particular, let's consider a training sample—corresponding to a certain set of PUs with given transmit powers, PURs, and SU S_i with allocated power Π which satisfies Eqn. 1.¹ (Our discussion in this subsection applies to both settings, viz., PU-Setting and SS-Setting.) Let l_i be the location of the SU S_i . Now, let PUR R_j be the PUR that results in S_i 's allocated power, i.e., let $j = \arg \min_j \frac{\tau_j - l_j}{\rho(l_i, l_j)}$ from Eqn. 1. In the following discussion, we vary l_i while keeping everything else constant—thus, we can look at j , R_j and allocated

power Π as functions of l_i . Now, in a sufficiently small neighborhood N of S_i , the PUR $R_j(l_i)$ as computed above and thus $\Pi(l_i)$ must remain fixed for $l_i \in N$. Moreover, $\Pi(l_i)$ is also inversely proportion to $\rho(l_i, l_j)$ with l_j fixed, and more importantly, variation of $\Pi(l_i)$ within N is largely dominated by the small-scale effect of the path-loss function. Let $y = \max_{l_i \in N} \Pi(l_i) - \min_{l_i \in N} \Pi(l_i)$, which in some sense is an estimate of the "amplitude" of the small-scale effect. We now use the value of y to lower the allocated power label of the training samples. See Fig. 5(b). The modified samples essentially correspond to a conservative spectrum allocation function, without the small scale effect. Note that the value y depends on the small-scale effect of the terrain. If we assume the effect to be uniform across the given region, then the same value of y can be used across all the training samples—else, we compute y in each subarea.

3.5 Synthetic Samples to Improve Performance

One way to improve performance, i.e., to aid the model in extracting the most information from the given training samples, is to create additional *synthetic* samples from the training samples. In effect, the new synthetic samples incorporate the domain knowledge used in creating them. In general, from a given sample $\{X, y\}$ where X is the set of features (PU parameters or SS readings, and the

¹However, note that Π is not computed using Eqn. 1, as many terms in it are unavailable.

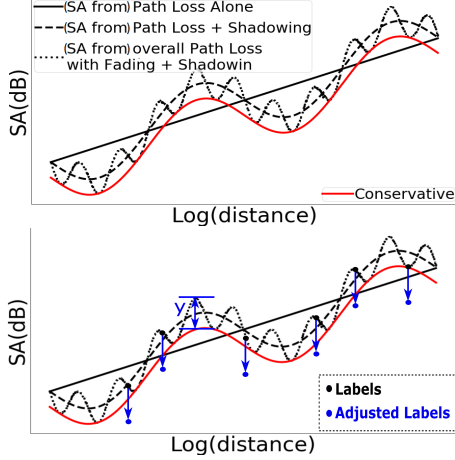


Figure 5: (a) Spectrum allocation function, when there is a single PU and a single SU, due to path-loss with shadowing and multi-path fading effects. Note that the path-loss function has a similar trend. The red plot is a conservative spectrum allocation, based on a similar conservative path-loss function. (b) Modifying labels of training samples to drive the model towards learning a simpler and more conservative spectrum allocation function.

requesting SU’s location) and y is the label (allocated power), we create synthetic samples of the type $\{X', y\}$ where X' is another set of features that yields (approximately) the same label y . Below, we discuss the generation of synthetic samples for our two settings.

PU-Setting. Consider a sample $\{X, y\}$ where X includes the PU parameters. For this sample, let P be the PU for the PUR R_j that determines the SU’s optimal power allocation, as in previous subsection. Let \mathcal{P} be a set of PUs that are sufficiently far away from P . Note that P is determined when labeling the given sample, and \mathcal{P} can be determined from P and the available PU parameters. Now, note that decreasing the power of PUs in \mathcal{P} should not change the optimal power allocated to SU. Thus, we can create additional synthetic samples by considering X' which differs from X in that the transmit powers of PUs in \mathcal{P} is lower than that in X .

SS-Setting. In the setting, wherein the features are composed of sensor readings, we generate synthetic samples by determining sensor readings at additional locations via interpolation techniques. In particular, based on the log-distance like behavior of signal attenuation, we use a slight modification of the traditional IDW technique. More formally, for a known set of sensor readings (p_i, l_i) where p_i is the received power at location l_i , the interpolated value q at a new location l is given by: $q = \frac{\sum_i w_i p_i}{\sum_i w_i}$, where w_i is the weight defined as $w_i = \frac{1}{\log_{10}(d(l, l_i))}$. Based on the above interpolation scheme, for a given sample (X, y) where X is the set of real sensor readings, we can create synthetic samples of the type (X', y) where X' consists of some readings from X and some interpolated readings.

Rotated Images. In addition to above, we also synthesize additional samples by just “rotating” the images of the original samples; such a strategy is bound to be useful in regions where the propagation model is largely dependent on the distance. In our evaluations, we rotate the given images by 90 or 180 degrees.

3.6 Multiple SUs

Till now, we have only considered spectrum allocation to the initial single SU. Handling *subsequent* SUs in the same manner as the initial SU above requires the *updated* threshold values at PUR; for now, we focus on handling SUs *one at a time* (we discuss handling *simultaneous* SUs momentarily). One possible way to handle subsequent SUs is to augment the list of features to include the active SUs’ parameters, and train the model accordingly. This approach is viable, especially in the context of our DeepAlloc model, since active SUs with their parameters (location and allocated power) can easily be represented in the single input sheet dedicated to SUs. The only change we need to make is that we must now represent SU’s allocated power too; we can represent them with a disk similar to PUs, i.e., with the center’s brightness and radius proportional to the allocated power. The other ML techniques can also be similarly extended to handle subsequent SUs one at a time.

DeepAlloc-Greedy for Multiple SUs. When multiple SUs requests arrive *simultaneously*, we propose to still handle them one at a time. One simple way is to handle them one at a time in random order and allocate each request the optimal power possible; we refer to this as DeepAlloc-Random. Another way is to handle them in a greedy manner as described below; we refer to this as DeepAlloc-Greedy. First, we divide the whole area into non-overlapping subarea, and assign each subarea X a weighted score equal to the total aggregated power transmitting from all the PUs and active SUs in X or its adjoining cells. Then, we pick the SU requests in the ascending order of the weight of the subarea they belong to.

DeepAlloc-Fair for Fair Allocation. As DeepAlloc-Greedy tries to allocate the maximum power possible to a requesting SU, some SUs may not be allocated any power (e.g., if they are located near an SU already allocated optimal power). To address this unfairness issue for simultaneous multiple SUs, we modify the DeepAlloc-Greedy approach as follows to design a fair scheme DeepAlloc-Fair. If the allocated power to the requesting SU x is less than a certain threshold, then we “backtrack” and reduce the allocated power of some of the previously-allocated SUs. In particular, we reduce the power of the SUs “near” x in proportion to their individual impact in improving the power allocation to x ; we skip tedious details. This results in “freeing” up some spectrum for allocation to x . Note that, the low power allocation to x could also be due to it being very close to some PUs, in which case nothing can be done.

Multiple Channels; Request Durations. Till now, we have implicitly assumed a single channel. To handle multiple channels, we can extend our schemes easily. If the signal propagation characteristics are different for different channels, then we can create a separate model for each channel. Then, for a single-SU request, we can pick the channel that allows for maximum power allocation, while for multiple SUs, we can modify the above approaches DeepAlloc-Greedy and DeepAlloc-Fair easily for the multiple channels setting. The DeepAlloc-Greedy approach extends naturally. For the DeepAlloc-Fair approach, instead of just reducing powers of previously-allocated SUs, we can also consider the option of channel-reassignment, but for simplicity, we do not change assigned channels. Finally, to handle requests for a specified duration, we reallocate active requests whenever an SU becomes inactive (i.e., at the end of its request duration).

4 LARGE-SCALE SIMULATIONS

In this section, we discuss our large-scale simulation results conducted over a large geographical area (we discuss an outdoor testbed evaluation in the next section). We start with describing the underlying propagation model used in our simulations.

Longley-Rice Propagation Model and Setting. To evaluate our techniques over a realistic propagation model, we use the well-known Longley-Rice [12] Irregular Terrain With Obstruction Model (ITWOM), which is a complex model of wireless propagation based on many parameters including locations, terrain data, obstructions, soil conditions, etc. We use SPLAT! [29] to generate path-loss values; SPLAT! is an open-source software implementing the Longley-Rice propagation model. When simulating the above propagation model, we consider an area of $1\text{ km} \times 1\text{ km}$ in our state and use the 600 MHz band to generate path losses using SPLAT!. As the height of an entity is an important factor in determining the path loss, we place the transmitters (PU or SU) at a height of 30m and the receivers (PURs and SSs) at 15m above the ground level. For clarity of presentation and due to limited space, in many plots, we only show results for the PU-Setting; in these cases, the observed trend in SS-Setting is similar.

Performance Metrics (\mathcal{A}_{err} , \mathcal{A}_{fp}) and Algorithms. The main performance metric used to evaluate our technique is the average (absolute) difference in power allocated to the requesting SU with respect to an optimal algorithm; here, the optimal algorithm has the knowledge of the exact path-loss values and is thus able to use the Eqn. 1 to compute the power to be allocated to the SU. We denote this measure by \mathcal{A}_{err} . To evaluate the impact of false positives, we also consider the average false-positive error metric \mathcal{A}_{fp} which is computed as the aggregate error in the false-positive samples over the false positives divided by the total number of samples. The \mathcal{A}_{fp} metric informally measures the level of interference caused by the spectrum allocations. We implement standard ML techniques, viz., a 3-layered neural network (NN), support vector regression (SVR) [18], our CNN-based approaches SH-Alloc (§3.1) and DeepAlloc (§3.2). Recall that DeepAlloc is based on a pre-trained deep CNN architecture. As detailed in §2, the closest work relevant to our setting is the one in [21] which has available the PUs’ parameter values as well as the SS readings, and uses interpolation techniques to estimate path-loss values between relevant entities; we denote this approach by IP-Based.² We note that the simple Listen-Before-Talk approach resulted in a \mathcal{A}_{err} of a several 10s of dB in our simulations, and has not been shown in the plots for clarity. The large \mathcal{A}_{err} value for the very conservative Listen-Before-Talk approach (see §2.1) is due to the fact that in a large majority of evaluation samples SU is not allocated *any* spectrum power as some of the PUs’ power is always received in a large fraction of the area.

Training Samples. As described in §3, there are two types of training samples used in training our models: (i) pre-training samples used to pre-train the DeepAlloc; these samples are based on the log-normal propagation model with a path-exponent computed from a small number of path-loss samples; we computed an exponent of 3.3 from 200 path-loss samples. (ii) *training samples*, which are gathered in the field as described below; these samples are used to

²In our implementation of IP-Based algorithm, we fine-tuned its internal path-loss exponent parameter α to get the best performance; we ended up using a value of 3.3.

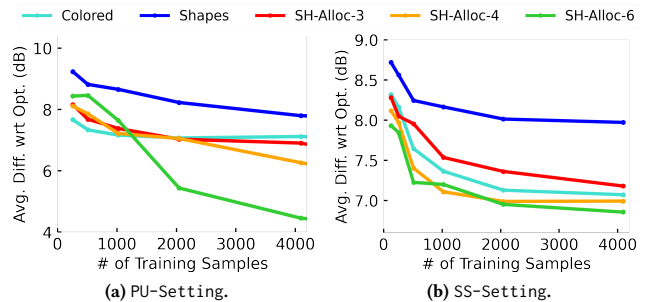


Figure 6: Performance comparison of various schemes for pre-processing the training samples into images.

train all the ML models, including the DeepAlloc after pre-training. In addition, for our schemes, we also use synthetic samples (§3.5), which are derived from the training samples. In most of our plots, we vary the total number of training samples from 256 to about 4096 (with default value of 2048), of which 20% are used for validation purposes (to tune the model’s hyper-parameters) and the remaining are used to train the model. In addition, we create and use 40,000 separate samples for evaluation purposes. To create a training/evaluation sample, we place 10 to 20 PUs at random locations in the given area and assign them a random power within the range of 0 to -30dBm. Each PU has a random number (5 to 10) of PURs distributed randomly within a distance of 50m from the PU. We vary the number of sensors from 400 to 3600 (with 1600 as the default) sensors uniformly distributed in the field. For NN and SVR models, we assume the maximum number of PUs to be 20, and use dummy parameter values if the number is less than 20.

4.1 Performance Results (Single SU)

We now present our performance results for various algorithms and settings. We evaluate various techniques for the case of a single SU request; we consider multiple SUs in the next subsection.

Various Pre-Processing Schemes. We start with evaluating various pre-processing schemes of creating images from the training samples, as input to our basic CNN approach SH-Alloc. Here, we refer to the multi-sheets based approaches (i.e., from Fig. 2) as SH-Alloc- N , where N is the number of sheets used for the PUs/SSs. We also evaluate the Colored and Shapes schemes, where the Colored scheme uses different colored-disks (red, green, and blue) for the three entities (PU, SS, and SU) and the Shapes scheme uses a grayscale image with different shapes for the entities (PU: circle, SU: square, SS: rectangle). We maintain the shape sizes to be small (to avoid intersection) and uniform for each entity, but vary the intensity to represent the transmitted (received) power. See Fig. 6 for a performance comparison of the above schemes in both settings. We observe that the SH-Alloc- N schemes outperform the other two schemes, with the increase in N improving the performance as expected. Thus, we use 6 image sheets for PUs/SSs.

Varying Training Cost and Number of PUs/SSs. We now evaluate the fundamental performance of various algorithms in terms of the key \mathcal{A}_{err} metric in our two settings, PU-Setting and SS-Setting, for varying number of (field-gathered) training samples and number of PUs/SSs. See Fig. 7. First, our main DeepAlloc approach outperforms all the other approaches for both settings. More importantly,

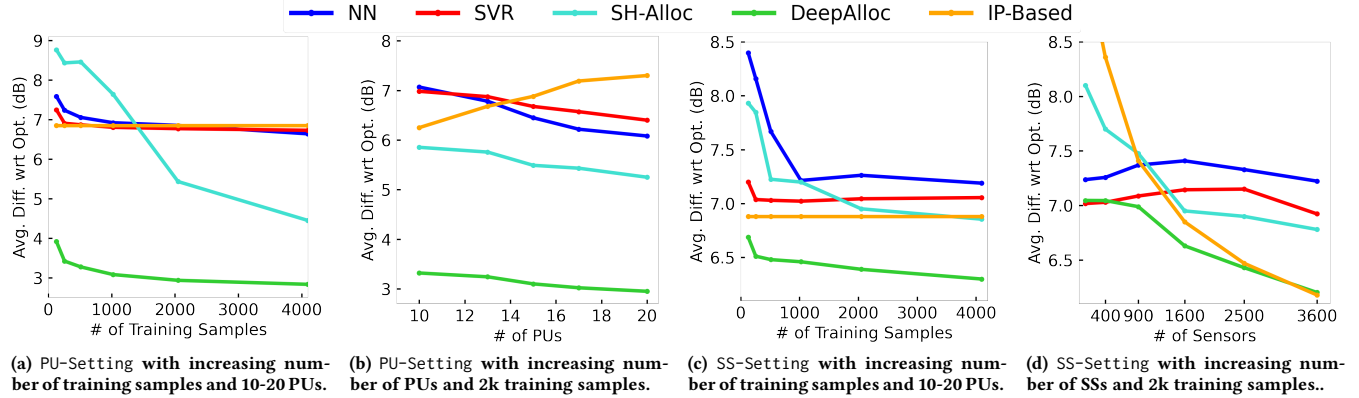


Figure 7: Performance comparison of various algorithms for increasing number of training samples and PUs/SSs.

DeepAlloc delivers great performance for the PU-Setting with less than 3dB performance gap with the optimal solution. As expected, the performance of our approaches is better in PU-Setting than that in SS-Setting, since fundamentally the PU-Setting has more direct information relevant to the spectrum allocation function. Second and more specifically, we observe that both the CNN-based approaches outperform the IP-Based algorithm by a large margin in the PU-Setting; in the SS-Setting, the DeepAlloc approach easily outperforms the IP-Based algorithm, except for large number of sensors wherein both techniques perform similarly. Recall that the IP-Based approach has the advantage of knowing *both* the PU parameters as well as SS readings, while the ML algorithms have knowledge of only one of these inputs—thus, it is surprising and commendable that DeepAlloc is able to outperform the IP-Based approach. Above observations suggest that DeepAlloc is able to learn the spectrum allocation function effectively. Lastly, we observe that the performance gap between the CNN-based approaches (SH-Alloc and DeepAlloc) is significant—which demonstrates the value of pre-training a deep CNN model.

Evaluating Techniques for Minimizing False-Positive Errors, Handing Multi-Path Effect, and Synthetic Samples. We now evaluate our specialized techniques developed in §3.3-3.5 for various aspects. See Fig. 8. Fig. 8(a) evaluates the §3.4’s technique to minimize false positives. We plot \mathcal{A}_{err} and \mathcal{A}_{fp} metrics for varying $\alpha_{\text{FP}}/\alpha_{\text{FN}}$ ratio; we see that increase in $\alpha_{\text{FP}}/\alpha_{\text{FN}}$ ratio is effective in minimizing the false-positive error \mathcal{A}_{fp} , at the cost of higher average \mathcal{A}_{err} . Next, in Fig. 8(b), we evaluate the technique from §3.4 to handle multi-path fading effects by learning a conservative function via modified labels. Here, we plot the \mathcal{A}_{err} and \mathcal{A}_{fp} for the basic as well as the conservative technique. We observe that the conservative technique’s false-positive error (\mathcal{A}_{fp}) is indeed reduced without much increase in the total error (\mathcal{A}_{err}), compared to the basic approach. Fig. 8(a)-(b) are in PU-Setting; the SS-Setting results were similar (not shown). Finally, in Fig. 8(c)-(d), we evaluate the benefit of using synthetic samples as described in §3.5. Here, we show PU-Setting as well as SS-Setting as the algorithms for generating synthetic samples are very different. In PU-Setting (Fig. 8(c)), the performance gain due to synthetic samples is positive but minimal—perhaps, because the performance was already near-optimal. In SS-Setting (Fig. 8(d)), we see a significant performance improvement due to synthetic samples—validating our use of interpolation-based synthetic samples. Here, we added 2500 new

uniformly-distributed sensors and interpolate their readings using the four nearest original sensors.

Multiple Regions. We also evaluated our DeepAlloc scheme over other regions with different sizes and terrain characteristics. See Fig. 9(a), which plots performance of DeepAlloc over three different regions— $500m \times 500m$ (our university campus), $1km \times 1km$ (airport landing area, the default region in all other plots), and $5km \times 5km$ (an urban area). We plot results for PU-Setting wherein the number of PUs is between 10 and 20. We see that DeepAlloc has an \mathcal{A}_{err} of 3-4.5 dB across all regions, and it performs the best over the airport landing area likely due to lack of buildings and thus more uniform path-loss characteristics.

Various Pre-Trained Models. Finally, we present evaluation results for various pre-trained deep models. In particular, in addition to our DeepAlloc architecture, we also used some well-known Image Classification models such as VGG [36], ResNet [22], and Xception [14] which are all pre-trained with over 1 million images (from ImageNet [16]) involving our daily-life objects (rather than spectrum allocation samples, as in DeepAlloc) and thus, their models are likely not perfectly tuned to our setting. See Fig. 9(b), which plots the \mathcal{A}_{err} metric in PU-Setting for the above pre-trained models each then trained with varying number of (field-gathered) training samples.³ We see that our approach of pre-training using log-normal model based images in DeepAlloc yields a notable performance improvement; the performance gap is significant for lower number of training samples.

4.2 Multiple SUs/Channels

We now present evaluation results for the general case of multiple SUs and/or channels setting.

Multiple SUs. We start with comparing the spectrum power allocated to a *single* new SU with previous SUs being active. Each sample has a random number (between 1 and 10) of active SUs. For evaluation purposes, we assume that the active SUs are assigned the optimal power (as per Eqn. 1, with full knowledge of PU information and path-loss values) and they transmit using this optimal power. Then, the models predict the allocation power for the last requesting SU. See Fig. 10(a), which shows the performance of various ML algorithms in assigning the power to the last SU. We see

³For other pre-trained models, we use Colored scheme of creating images from training images, as they use colored images (rather than sheets) during pre-training.

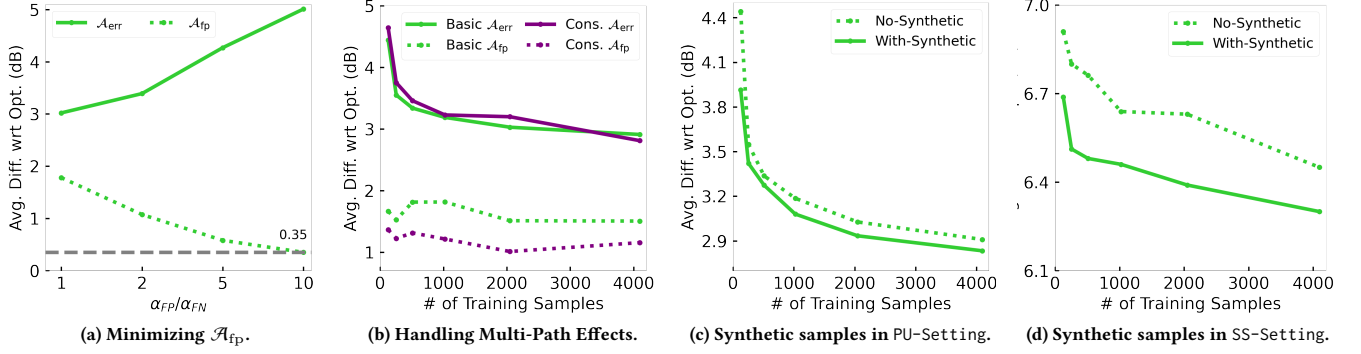


Figure 8: (a) Minimizing false-positive error (\mathcal{A}_{fp}), (b) Handling multi-path effect via learning a more conservative function, and (c)-(d) Using synthetic samples to improve performance. Here, (a)-(b) are in PU-Setting; the SS-Setting had similar results.

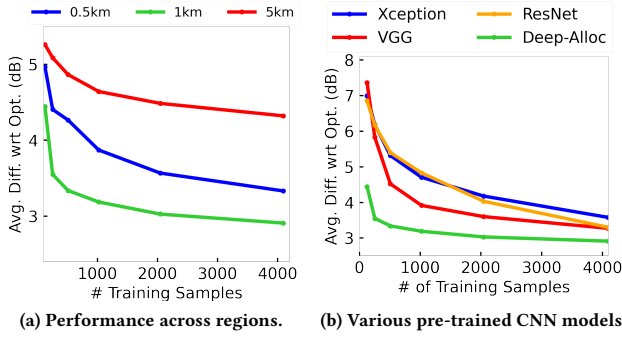


Figure 9: Performance comparison of (a) DeepAlloc over different regions, and (b) various pre-trained models for increasing number of training samples.

that DeepAlloc easily outperforms the other ML approaches by a large margin. Also, not shown for clarity, but IP-Based had a poor \mathcal{A}_{err} of 21.6dB and SH-Alloc had a \mathcal{A}_{err} 's of 7.5dB.

Total Power and Fairness Metric. Next, we compare the total allocated power and a fairness metric for our various multi-SU approaches (§3.6), viz., DeepAlloc-Random, DeepAlloc-Greedy, and DeepAlloc-Fair. We choose fairness metric of the ratio of maximum power allocated to an SU to the minimum power allocated to an SU; a lower value of this metric suggest fair allocation across the SUs. See Fig. 10(b)-(c). We observe that as desired the fair approach DeepAlloc-Fair has the best fairness metric, while having only a small disadvantage in the total power allocated. The greedy approach DeepAlloc-Greedy yields the highest total power allocated.

Spectrum Utilization (Data Rate). Finally, we compare the performance of our approaches in terms of the overall spectrum utilization which we model using achievable data rate as follows. For each SU, we assign a receiver in a random location around the SU, and estimate the data rate that can be achieved between the SU and the receiver in presence of the interference from PUs and other SUs. To compute achievable data rate, we calculate the SINR (signal-to-interference-plus-noise) ratio at the receiver, and use Shannon's capacity law to estimate the achievable data rate as $B \log_2(1 + \frac{S}{N+I})$ where B is the channel bandwidth (1MHz here), S is the average signal strength (received power), N is the average noise, and I is the interference. See Fig. 10(c), which plots the average data rate achieved by the SUs. As expected, we observe that the DeepAlloc-Greedy

approach performs the best, which validates our weighted-subarea based greedy approach. In this experiment, we moved the receiver to various locations around the SU within a distance of 100m.

Multiple Channels. In Fig. 11, we compare our multi-SU approaches (tailored to multiple channels as described in §3.6) in the 4-channel PU-Setting setting with PUs transmitting over all the channels at all times. We allocate powers to 30 SUs. We observe that DeepAlloc-Greedy still achieves the best performance in terms of total power allocation, and DeepAlloc-Fair has the best fairness metric. With respect to the single channel, the total power allocated is almost double.

5 DEEPALLOC TESTBED IMPLEMENTATION

In this section, we implement and evaluate a complete testbed system for our spectrum allocation system. We use the testbed to collect training samples, which are then used to train and evaluate the learned models. The testbed implementation demonstrates the effectiveness of our techniques in a realistic small-scale setting.

Transmitter and Receiver Devices Used. We use 4 USRP B200/B210 and 1 HackRF to play the role of the 4 PUs and 1 SU, respectively. A spectrum sensor (SS) is composed of an RTL-SDR dongle that connects to a dipole antenna and is powered by a single-board computer Odroid-C2. We deploy 17 of these spectrum sensors in the testbed. See Fig. 12(a). To simulate PU receivers (i.e., PURs), we use the same RTL-SDR dongle and antenna but power it by a laptop. Each PU is paired with one PUR, and they are both powered by a single laptop. Overall, we implemented a Python repository running on Linux which transmits and receives signals, and measure and collect relevant parameters in real-time at 915 MHz ISM band at a sample rate of 1 MHz. We built our custom communication system based on GNU Radio for data communication between PU and PURs, used to determine labels (see below). See Fig. 13.

Collecting Training Samples. Recall that a sample in PU-Setting is comprised of a sample of PUs' parameters (location and power) and the optimal power allocated to the SU. In SS-Setting, a training sample is comprised of spectrum sensors' received power readings. The location of entities is available by using a GPS dongle connected to the laptops as described below, and the sensor's received power is computed as follows. First, we compute an FFT on the I/Q samples collected within a time window to get a power spectral density (PSD) plot. Then, we compute the area under the

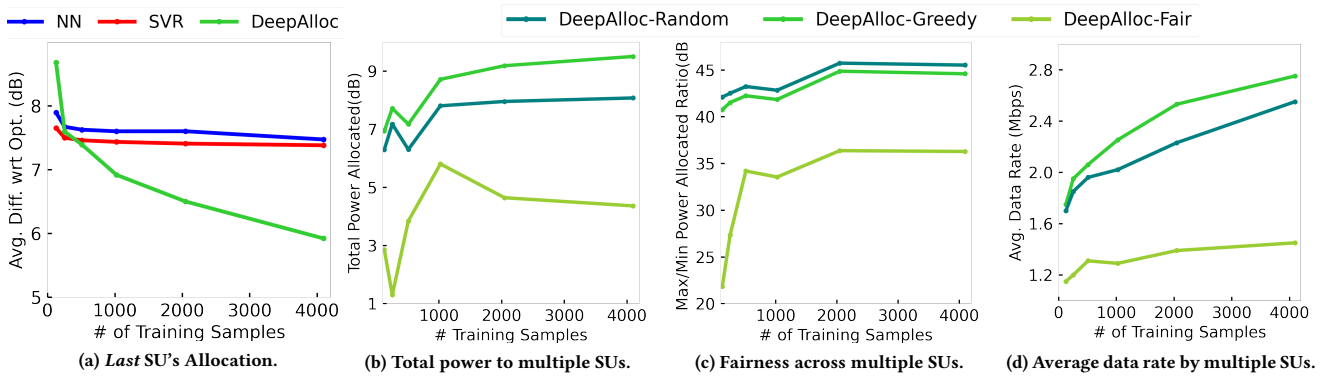


Figure 10: Spectrum Allocation to Multiple SUs. (a) Power allocated to subsequent SUs, in presence of other active SUs. (b)-(d) Total power allocated, Fairness (max/min ratio), and Total data rate for multiple SUs by various multi-SU algorithms.

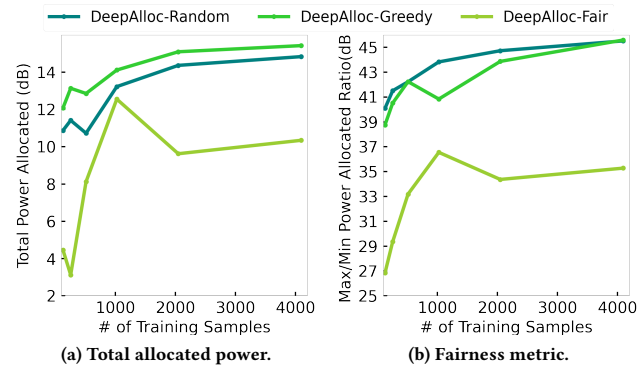


Figure 11: (a) Total allocated power, and (b) Fairness metric, in a four-channel setting with multiple SUs.

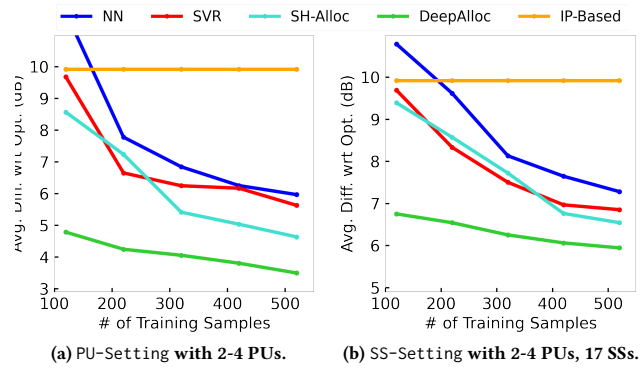


Figure 14: Testbed performance for increasing training set.

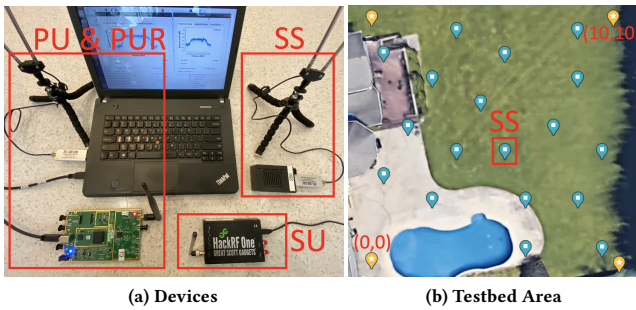


Figure 12: Outdoor testbed. (a) Devices for PU, PUR, SU, and SS; (b) The testbed area (a private house backyard). Blue stars are the 18 sensors.

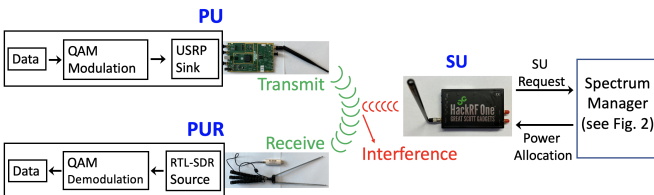


Figure 13: Testbed system overview, including the GNU-Radio based PU-to-PUR communication system .

PSD curve over the 1 MHz channel of interest (see below), and finally, convert the computed area to an appropriate unit.

Determining Labels (Optimal Power Allocated to SU). We essentially do a binary search to estimate the optimal power that can be allocated to SU. To determine whether PU to PUR transmission is incurring any harmful interference from SU, we have PU continuously streaming ASCII messages over the 1 MHz bandwidth channel centered at frequency 915.8 MHz, and check if the messages are successfully received at the PUR. This end-to-end communication system is implemented using GNU Radio.

Testbed Area and Setting. Due to the ongoing pandemic, the testbed was conducted in the backyard of a private house. The whole area is $24m \times 24m$ large. We divide the area into 100 grid cells where each represents $2.4m \times 2.4m$. See Figure 12(b). We use a GPS dongle that returns location in (latitude, longitude) and the program converts it into coordinates. We determine the location of PU, SU, and the sensors with the help of GPS dongles and manual observation. All the Odroids and laptops are connected to an outdoor WiFi router and communicate through ssh protocol. For training and evaluation, the 17 sensing devices are placed on the ground and are uniformly spread out. PUs and SU are randomly placed in the area such that different regions of the backyard are "covered". PUs' power is randomly assigned within a certain range.

Results. First, we evaluate the performance for an increasing number of training samples. See Fig. 14. We observe a similar trend as in the previous section of large-scale simulation, with DeepAlloc outperforming other algorithms with a notable margin. In particular, the overall performance of DeepAlloc is good, with 4-5dB

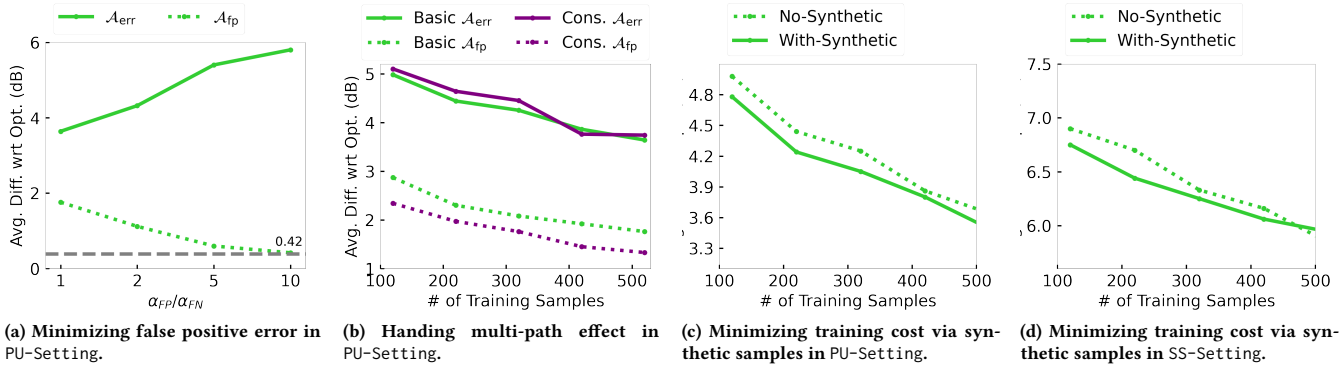


Figure 15: Evaluation of various aspects in the testbed.

error using only 500 training samples. The performance of all algorithms is better in PU-Setting relative to the SS-Setting, as in §4. Note that IP-Based performs quite poorly in this realistic setting, in spite of having knowledge of PU information as well as SS readings, as it assumes an imprecise propagation model. Finally, we evaluate our techniques to handle various aspects, viz., false positive error, multi-path effect, and synthetic samples in Fig. 15. Overall, we observe a similar trend as in the large-scale simulations.

6 CONCLUSIONS

We have motivated and developed an effective supervised learning technique based on CNNs to learn the spectrum allocation function. We demonstrate the effectiveness of our approach via extensive large-scale simulations as well as a small outdoor testbed. There are many avenues for further improvement of our techniques. First, one could easily pre-train the DeepAlloc model with a much larger number of pre-training samples; as our pre-training samples can be automatically generated, this only incurs additional computational cost but no additional field training/deployment cost. (ii) We could also use a more complex propagation model to generate the pre-training samples. (iii) Lastly, we could incorporate terrain information in the image sheets to aid the learning process. These directions form the focus of our future work.

REFERENCES

- [1] FCC 3.5GHz Band. <https://www.fcc.gov/wireless/bureau-divisions/mobility-division/35-ghz-band/35-ghz-band-overview>.
- [2] FCC White Space. <https://www.fcc.gov/general/white-space>.
- [3] Jeffrey G. Andrews, Stefano Buzzi, et al. What will 5g be? *IEEE Journal on Selected Areas in Communications*, 2014.
- [4] F. Azmat, Y. Chen, and N. Stocks. Analysis of spectrum occupancy using machine learning algorithms. *IEEE Transactions on Vehicular Technology*, Sep. 2016.
- [5] Yoshua Bengio, Ian Goodfellow, and Aaron Courville. *Deep learning*, volume 1. MIT press Massachusetts, USA:, 2017.
- [6] Sudeep Bhattarai et al. An overview of dynamic spectrum sharing: Ongoing initiatives, challenges, and a roadmap for future research. *IEEE TCCN*, 2016.
- [7] Milind M. Buddhikot et al. Dimsumnet: new directions in wireless networking using coordinated dynamic spectrum. In *IEEE WOWMOM*, June 2005.
- [8] S. Byun et al. Dynamic spectrum allocation in wireless cognitive sensor networks: Improving fairness and energy efficiency. In *IEEE VTC*, 2008.
- [9] Roberto Calvo-Palomino, Domenico Giustiniano, Vincent Lenders, and Aymen Fakhreddine. Crowdsourcing spectrum data decoding. In *IEEE INFOCOM*, 2017.
- [10] Ayon Chakraborty and Samir R. Das. Measurement-augmented spectrum databases for white space spectrum. In *CoNEXT*, 2014.
- [11] Ayon Chakraborty, M. S. Rahman, H. Gupta, and S. Das. Specsense: Crowdsensing for efficient querying of spectrum occupancy. In *IEEE INFOCOM*, 2017.
- [12] K. Chamberlin and R. Luebbers. An evaluation of longley-ricce and gtd propagation models. *IEEE Transactions on Antennas and Propagation*, November 1982.

- [13] Wentai Chen et al. A reinforcement learning based joint spectrum allocation and power control algorithm for d2d communication underlying cellular networks. In *AICON*, 2019.
- [14] F. Chollet. Xception: Deep learning with depthwise separable convolutions, 2017.
- [15] Max Curran, Xiao Liang, Himanshu Gupta, Omkant Pandey, and S. Das. Procsa: Protecting privacy in crowdsourced spectrum allocation. In *ESORICS*, 2019.
- [16] Jia Deng, Wei Dong, Richard Socher, Li-Jia Li, Kai Li, and Li Fei-Fei. Imagenet: A large-scale hierarchical image database. In *IEEE CVPR*, 2009.
- [17] Y. Dou, K. Zeng, et al. P^2 -SAS: Privacy-preserving centralized dynamic spectrum access system. *IEEE Journal on Selected Areas in Communications*, Jan 2017.
- [18] Harris Drucker, Christopher JC Burges, Linda Kaufman, Alex J Smola, and Vladimir Vapnik. Support vector regression machines. In *NeurIPS*, 1997.
- [19] M. El Tanab and W. Hamouda. Resource allocation for underlay cognitive radio networks: A survey. *IEEE Communications Surveys Tutorials*, 2017.
- [20] S. Gao, L. Qian, and D. R. Vaman. Distributed energy efficient spectrum access in wireless cognitive radio sensor networks. In *WCNC*, 2008.
- [21] H. Gupta, M. Rahman, and M. Curran. Shared spectrum allocation via pathloss estimation in crowdsensed shared spectrum systems. In *DySPAN*, Nov 2019.
- [22] Kaimeing He, Xiangyu Zhang, Shaoqing Ren, and Jian Sun. Deep residual learning for image recognition. In *IEEE CVPR*, 2016.
- [23] S. He, D. Shin, J. Zhang, and J. Chen. Toward optimal allocation of location dependent tasks in crowdsensing. In *IEEE INFOCOM*, 2014.
- [24] A. T. Hoang et al. Power control and channel allocation in cognitive radio networks with primary users' cooperation. *IEEE TMC*, March 2010.
- [25] P. Karimi, W. Lehr, I. Seskar, and D. Raychaudhuri. Smap: A scalable and distributed architecture for dynamic spectrum management. In *DySPAN*, Oct 2018.
- [26] W. Lee and I. F. Akylidiz. A spectrum decision framework for cognitive radio networks. *IEEE Transactions on Mobile Computing*, 2011.
- [27] Alexe E Leu et al. Modeling and analysis of interference in listen-before-talk spectrum access schemes. *International Journal of Network Management*, 2006.
- [28] Xiukui Li and Seyed A. (Reza) Zekavat. Distributed channel assignment in cognitive radio networks. In *IWCNC*, 2009.
- [29] J. A. Magliacane. Splat! a terrestrial rf path analysis application for linux/unix. Downloaded from <https://www.qsl.net/kd2bd/splat.html>, 2008.
- [30] A. Medeisis and A. Kajakas. On the use of the universal okumura-hata propagation prediction model in rural areas. In *IEEE VTC*, May 2000.
- [31] Nils Morozs. *Accelerating Reinforcement Learning for Dynamic Spectrum Access in Cognitive Wireless Networks*. PhD thesis, University of York, 2015.
- [32] Vinod Nair and Geoffrey E Hinton. Rectified linear units improve restricted boltzmann machines. In *ICML*, 2010.
- [33] H. Salameh. Throughput-oriented channel assignment for opportunistic spectrum access networks. *Mathematical and Computer Modelling*, 2011.
- [34] P Mohana Shankar. *Fading and shadowing in wireless systems*. Springer, 2017.
- [35] J. Shi, Z. Guan, C. Qiao, T. Melodia, G. Challen, et al. Crowdsourcing access network spectrum allocation using smartphones. In *HotNets*, 2014.
- [36] Karen Simonyan and Andrew Zisserman. Very deep convolutional networks for large-scale image recognition. In *ICLR*, 2015.
- [37] Y. Song, K. W. Sung, and Y. Han. Coexistence of wi-fi and cellular with listen-before-talk in unlicensed spectrum. *IEEE Communications Letters*, 2016.
- [38] E. Z. Tragos et al. Spectrum assignment in cognitive radio networks: A comprehensive survey. *IEEE Communications Surveys Tutorials*, 2013.
- [39] M. Uccellari, F. Facchini, et al. On the application of support vector machines to the prediction of propagation losses at 169mhz for smart metering applications. *IET Microwaves, Antennas Propagation*, 2018.
- [40] H. Wang, J. Ren, and T. Li. Resource allocation with load balancing for cognitive radio networks. In *GlobCom*, 2010.
- [41] W. Wang, K. G. Shin, and W. Wang. Joint spectrum allocation and power control for multihop cognitive radio networks. *IEEE TMC*, 2011.

- [42] Yonghua Wang et al. A survey of dynamic spectrum allocation based on reinforcement learning algorithms in cognitive radio networks. *AIR*, 2019.
- [43] L. Yu, C. Liu, and W. Hu. Spectrum allocation algorithm in cognitive ad-hoc networks with high energy efficiency. In *ICGCS*, 2010.
- [44] Caitao Zhan, Mohammad Ghaderibaneh, Pranjal Sahu, and Himanshu Gupta. Deepmtl: Deep learning based multiple transmitter localization. In *2021 IEEE 22nd International Symposium on a World of Wireless, Mobile and Multimedia Networks (WoWMoM)*, pages 41–50, 2021.
- [45] H. Zhang, N. Yang, W. Huangfu, K. Long, and V. C. M. Leung. Power control based on deep reinforcement learning for spectrum sharing. *IEEE TWC*, 2020.
- [46] Q. Zhao and B. M. Sadler. A survey of dynamic spectrum access. *IEEE Signal Processing Magazine*, 2007.
- [47] Z. Zhao, P. Zheng, S. Xu, and X. Wu. Object detection with deep learning: A review. *IEEE Transactions on Neural Networks and Learning Systems*, 2019.